1. Yashar EMAMI [1], 2. Amangaldi KOOCHAKI [2*], 3.Masoud RADMEHR[3]

Department of Electrical Engineering, Aliabad Katoul Branch, Islamic Azad University, Aliabad Katoul, Iran (1,2,3)
ORCID: 1. 0000-0001-7004-3311; 2. 0000-0001-6841-534X; 3. 0000-0003-3720-8318

doi:10.15199/48.2024.05.47

Mitigation Sub synchronous Resonance and Improvement Low-Voltage Ride-Through Capability of Series Compensated Doubly-Fed Induction Machine Based Wind Farms by Using Bridge-Type Solid-State FCL

Abstract. *Series-Capacitor compensation approach is widely used in transmission lines to expand the active power capacity of transmission lines. They provides a practical solution for Connection large-scale wind farms (WFs) to grid in order to transmit the wind power to grids in long distance load centres. Integration large-scale WFs to power system may lead to sub synchronous resonance (SSR) phenomenon and low-voltage ride through (LVRT) challenges in WFs connected through series capacitive compensated transmission lines. This paper suggest the employment of bridge-type solid-state fault current limiter (BSFCL) for damping the SSR and enhancing the LVRT performance of series capacitive compensated WFs integrated to power system. The WF modelled in this study is an aggregated doubly fed induction machine (DFIM). The first standard benchmark IEEE system is modified and is simulated in PSCAD/EMTDC software to show the BSFCL capability for damping the SSR and improving the LVRT requirements of WFs in this paper. Considering simulation results, it is found that the BSFCL effectively mitigates the SSR oscillations and fulfils the LVRT requirement of series capacitive compensated WF integrated to power system.*

Streszczenie. *Metoda kompensacji szeregowo-kondensatorowej jest szeroko stosowana w liniach przesyłowych w celu zwiększenia mocy czynnej linii przesyłowych. Zapewniają praktyczne rozwiązanie umożliwiające podłączenie dużych farm wiatrowych (FW) do sieci w celu przesyłania energii wiatrowej do sieci w dalekobieżnych ośrodkach obciążenia. Integracja wielkoskalowych FW z systemem elektroenergetycznym może prowadzić do zjawiska rezonansu podsynchronicznego (SSR) i wyzwań związanych z przechodzeniem niskiego napięcia (LVRT) w FW połączonych szeregowymi, kompensowanymi pojemnościowo liniami przesyłowymi. W artykule tym zasugerowano zastosowanie półprzewodnikowego ogranicznika prądu zwarciowego typu mostkowego (BSFCL) do tłumienia SSR i zwiększania wydajności LVRT szeregowych WF z kompensacją pojemnościową zintegrowanych z systemem zasilania. WF modelowany w tym badaniu to zagregowana maszyna indukcyjna z podwójnym zasilaniem (DFIM). W tym artykule pierwszy standardowy system wzorcowy IEEE został zmodyfikowany i symulowany w oprogramowaniu PSCAD/EMTDC w celu pokazania zdolności BSFCL do tłumienia SSR i poprawy wymagań LVRT dla WF. Biorąc pod uwagę wyniki symulacji, stwierdzono, że BSFCL skutecznie łagodzi oscylacje SSR i spełnia wymagania LVRT dla szeregowego FW z kompensacją pojemnościową zintegrowanego z systemem zasilania. (**Łagodzenie rezonansu podsynchronicznego i poprawa zdolności przejazdu przy niskim napięciu w farmach wiatrowych opartych na maszynach indukcyjnych z kompensacją szeregową, podwójnie zasilanych, poprzez zastosowanie półprzewodnikowego FCL typu mostkowego**)*

Keywords: Wind Farms, LVRT, SSR, DFIM, BSFCL
Słowa kluczowe: Farmy wiatrowe, LVRT, SSR, DFIM, BSFC

Introduction

Escalating the contribution and transmission of wind-power are two main challenges of WFs connected to power grid. Generally, WFs are far from load centres and require long transmission lines to transmit the wind power to them. Compensation transmission line by series capacitors is a practical approach to increase the transmission lines power transfer capacity for long distance [1]. However, the application of series capacitors may causes to occur the sub-synchronous resonance (SSR) in WFs [2]. In addition, using the series capacitor reduces the transmission impedance and cause to increase the WF fault current during short-circuit faults [1-2]. SSR in WFs cause to increase the energy exchange with power system and generator shaft at one or more sub synchronous frequencies, which may load to failure of wind turbines and subsequently disconnection from power system unlike the WF integration grid codes. Based on the LVRT requirements, WFs must remain in-service in during different faults to guarantee the power system stability [3].SSR events in WFs are classified in to self-excitation and transient SSR events. The details of both SSR events are presented in references [2-3].

In 2009, large number wind turbines of WFs were destroyed due to a SSR incident in southern Texas. USA [4]. In 2012, this phenomenon was repeated at the WF in the Guyuan area of china. In 2017 from August to October, three SSR circumstances were occurred in Texas. USA. All of these were occurred in the DFIMs-based series compensated WFs connected to power systems.

There are two approaches to mitigate the SSR in DFIM-based WFs including using the hardware additional flexible AC transmission systems (FACTs) devices and the software modification control of DFIM converters [5]. Application of different types of shunt and series FACTs devices is the prominent approach to control the SSR events in WFs [4-5]. In [5]-[6], the static VAR compensator (SVC) is used to mitigate the SSR in DFIM-based WFs. Gate-controlled series capacitor (GCSC) is one of well-known series controllers, which is used for suppressing the SSR in WFs [7-8]. In ref [7], it is suggested to use instead of the fixed capacitor. In [8], the authors of ref [8], a damping controller has been proposed and incorporate to the GCSC to control the SSR events in WFs. In [9], the fuzzy-logic controller (FLC) method is used to obtain the different gains of GSCS supplementary damping controller to increase the active power capacity of transmission lines and suppress the SSR events simultaneously. In [10], the unified power flow controller (UPFC) is used for controlling the SSR in series-capacitor compensated WFs. In [11], a designed supplementary damping controller based on model control theory is incorporated to the UPFC for damping the SSR events in WFs. In this study a hybrid generation-system includes steam turbine-based and DFIM-based power plants is used. In [12], a dual-functional FCL is proposed, which can provide variable series capacitor to compensate the transmission line and damp the SSR in WFs.

In [13], authors a new supplementary damping controller has been designed to integrate the thyristor controlled series capacitor (TCSC). This approach provides an efficient result for reducing the SSR phenomenon. In [14], the performance of TCSC and SVC for suppressing the

SSR events have been compared. Simulation results was shown that the application of TCSC in WF is efficient for controlling the SSR . In [15], the static-synchronous compensator (STATCOM) is another FACTS controller, which has been used for damping the SSR in series compensated WFs. In [16], a supplementary -damping controller was designed to integrate the STATCOM for SSR mitigating. Reference [17], the static-synchronous series compensator (SSSC) with an auxiliary SSR damping controller is suggested to damp the SSR in WFs. In [18], Bypass filters are used for damping the SSR in WFs.

Another challenge of compensation transmission lines by series capacitors in WFs, is their impedance decline. It increases the short circuit current level and has negative effect on the LVRT capability of WFs [19-20]. LVRT is the main requirement for connecting WFs to grid. It has become more important due to the augmenting penetration of wind-power into the existing power system.

According to the LVRT requirement, WFs must withstand the grid voltage sag and remain connected under fault conditions [21]. In researches, the application of FCLs have been recognized as an efficient approach to overcome these challenges [22]. The applications of FCLs, not only reduces the WFs fault current contribution, but also reduces the WF connecting point voltage. This characteristics of FCLs effectively fulfills the LVRT requirement of WFs [23]. Generally, FCLs are classified into solid-state type [24-25], superconducting type [26] and LC series [27], and parallel [28], resonance type, which are used in both DC and AC grids [29]. BSFCLs incorporated by DC reactors are promising solution and getting more acceptance for installation in WFs [30]. It can provide a controllable impedance for connection WFs to AC grid.

Considering the mentioned background, this paper uses the BSFCL for mitigating the SSR events in the series-capacitor compensated doubly fed induction machine (DFIM)-based WFs. To verify the performance of BSFCL for mitigating the SSR in DFIM-based WFs, the PSCAD/EMTDC software is used.

Studied System Model

To present the BSFCL capability for damping the SSR in WFs, the first standard benchmark IEEE system has been modified according to Fig. 1. The simulated WF in this study includes 100*2MW, which is modelled by an aggregated DFIM driven by a 200MW wind turbine. The studied WF is incorporated to the grid through a compensated single transmission-line by series capacitor and the SBFCL. The grid is modelled by Thethevenin equivalent circuit model include a series voltage-source and impedance, which are defined by *Vg* and *Zg* respectively. A three line-to-ground (LLLG) short circuit fault is applied in grid side of the studied system according to Fig. 1. The specifications of this system are presented in Table 1.

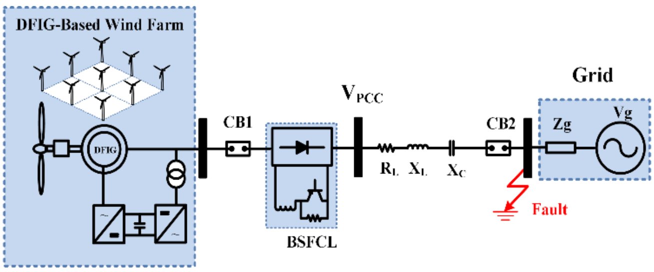

Fig. 1. Study modified IEEE first benchmark-system

DFIM-based Model

Fig. 2(a) shows different components of a DFIM type wind turbine. It includes an induction machine with wounded rotor configuration, two converters including the rotor side converter (RSC) and grid side converter (GSC), DC link capacitor and a wind turbine to drive the DFIM. According to the DFIM control system presented in Fig. 2(b), the RSC controls the output active power and reactive power of the DFIM through i_{qr} and i_{dr}, respectively. i_{qr} and i_{dr} are *q-axis* and *d-axis* components of the rotor currents. Also, the GSC control system regulates the DC link and PCC voltages in reference values. It is achieved this objective by i_{qs} and i_{ds}, respectively. i_{qs} and i_{ds} are the *q-axis* and *d-axis* components of the stator currents [31-32].The DFIM equivalent circuit is presented in Fig. 2. Equations (1)-(4) present the d-axis and q-axis components of the flux, and voltage equations of DFIM in the dq synchronous-reference frame as follows:

(1) $V_{dqs}=R_s i_{dqs}+\frac{d\lambda_{dqs}}{dt}-\omega_s\lambda_{dqs}$

(2) $V_{dqr}=R_r i_{qrdqr}+\frac{d\lambda_{dqr}}{dt}-(\omega_s-\omega_r)\lambda_{dqr}$

(3) $\lambda_{dqs}=L_s i_{dqs}+L_m i_{dqs}$

(4) $\lambda_{dqr}=L_s i_{dqr}+L_m i_{dqr}$

Table 1. Study system specifications

	Parameters Value	Parameters Value
Equivalent-Grid	Rated Voltage	230 kV
	Rated Frequency	50Hz
	The ratio of X and R	5
Induction Generator	Active power	2MW
	Voltage (L-L)	700V
	Frequency	50 Hz
	Inertia constant	1.2s
	Resistance of stator	0. 00565 Ω
	Leakage reactance of stator	0.0778 Ω
	Resistance of rotor	0. 0154 Ω
	Leakage reactance of rotor	0.1034Ω
	Mutual reactance	2.394 Ω
Transmission Lines	Reactance of line	0.33Ω/km
	Resistance of line	0.27Ω/km

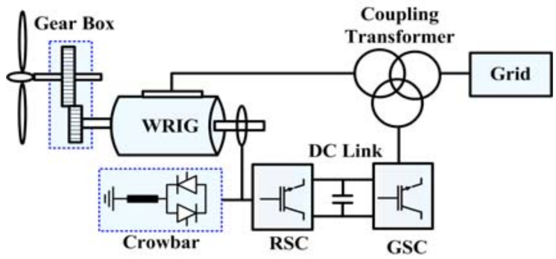

(a)

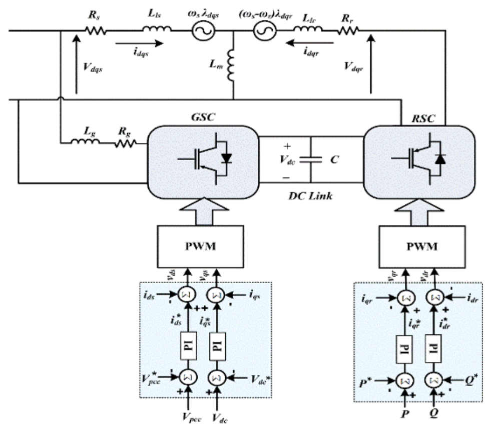

(b)

Fig. 2. DFIM, (a) power circuit, (b) Equivalent circuit and control system

In (1)-(4), $L_r= L_rL_m/(L_r+L_m)$ and $L_s= L_sL_m/(L_s+L_m)$. ω_r and ω_s are angular frequencies of the rotor and grid , respectively. Equations (5) and (6) presents the dynamic equations of GSC and DC link as follows:

(5) $$V_{dqs}=V_{dqg}+R_g i_{dqg}+L_g\frac{d\lambda_{dqg}}{dt}+\omega_s L_g i_{dqg}$$

and

(6) $$V_{dc}i_{dc}=P_g-P_r-P_{loss}$$

where, P_g and Q_g are:

(7) $$P_G=\frac{3}{2}\left(V_{QG}I_{QG}+V_{DG}I_{DG}\right)$$

(8) $$P_R=\frac{3}{2}\left(V_{QR}I_{QR}+V_{DR}I_{DR}\right)$$

The DFIM output active and reactive powers are expressed as follows:

(9) $$P_S=\frac{3}{2}\left(V_{qs}i_{qs}+V_{ds}i_{ds}\right)=-\frac{3}{2}\left(\frac{L_m}{L_S}V_{qs}i_{qr}\right)$$

(10) $$Q_S=\frac{3}{2}\left(V_{qs}i_{ds}-V_{ds}i_{qs}\right)=\frac{3}{2}\frac{L_m}{L_S}V_{qs}(i_{ms}-i_{dr})$$

Wind Turbine Model

To study the dynamic performance of wind turbine drive-train system, the two-mass shaft model is utilized from the PSCAD/EMTDC software library. The two-mass turbine model is presented in Fig. 3. It is modelled by following equations:

(11) $$\frac{\partial\omega_g}{\partial t}=\frac{1}{2H_g}(-T_e+K_{tg}\theta_{stgh}-D_{sh}(\omega_g-\omega_t))$$

(12) $$\frac{\partial\omega_t}{\partial t}=\frac{1}{2H_t}(-T_t-K_{tg}\theta_{tg})$$

(13) $$\frac{\partial\theta_{tg}}{\partial t}=(\omega_t-\omega_g)$$

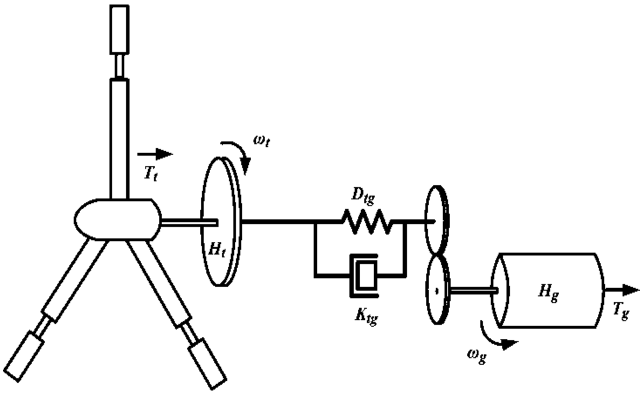

Fig. 3. Drive-train system

The mechanical torque relation with the wind speed is defined by following equation [33]:

(14) $$T_t=\frac{0.5\,A_w C_p(\lambda_c,\theta)v_w^3}{\omega_r}$$

In (14), T_t is the mechanical torque extracted from the wind turbine, ρ presents the air density, v_w presents the wind-speed, λ is the tip-speed ratio, A_w = πR^2, which R presents the radius blades, ω_r presents the angular mechanical-speed and C_P is the power coefficient. It is expressed by λ and θ , (pitch-angle)as follows:

(15) $$C_p(\lambda,\theta)=0.22(\frac{116}{\lambda_c}-0.4\theta-5)e^{-12.5\lambda_c}$$

(16) $$\lambda_c=\left(\frac{1}{\frac{1}{\lambda+0.08\theta}-\frac{0.035}{\theta^3-1}}\right)$$

Bridge-Type Solid-Sate FCL (BSFCL)

Fig. 4 demonstrates the circuit configuration of the BSFCL, which are composed by following parts:

1) A diode-bridge rectifier circuit contains D_1-D_4
2) An IGBT semiconductor switch (T)
3) A DC reactor to suppresses the instantaneous over current and the *di/dt in bridge circuit to protect the semiconductor switches*
4) A limiting-resistor (*R*) and,
5) A single-phase coupling transformer.

As shown in Fig. 4, the parallel limiting-resistor (R) and IGBT switch (T) are in series with the DC reactor. The DC reactor in this figure is modeled by rd and Ld. They represent the resistance and inductance of DC reactor.

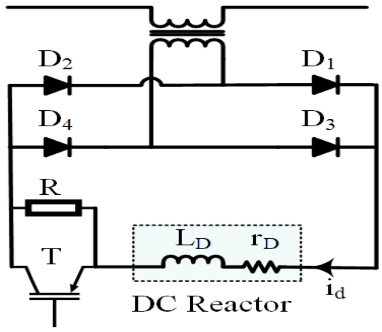

Fig. 4. Power circuit of BSFCL

Considering the grid condition, the IGBT switch operates in two states. When the grid condition is normal, the control system closes the T and under short-circuit fault condition in grid side, the T is opened. By changing the stat of T, two low-impedance (LI) and high-impedance path (HI) paths are made. The LI and HI paths carry the normal and fault condition currents, respectively. Fig 5(a) and (b) shows the LI path BSFCL equivalent circuit in normal condition for positive and negative cycle frequencies, respectively. Considering equivalent circuit in Fig. 5(a), the normal current flows by *D1-D4-L_D-r_D-T* path in positive half cycle. Fig. 5(b) demonstrates the current flow path in negative half cycle consists of *D2-D3-L_D-r_D-T* path. Fig 6(a) and (b) demonstrates the BSFCL high impedance path under fault condition for positive and negative half cycle frequencies, respectively. As demonstrated in Fig. 6(a), the fault current flows through *D1-D4-L_D-r_D-R* path in positive half cycle and *D1-D4-L_D-r_D-R* path in negative half cycle as demonstrated in Fig. 6(b). Under normal grid operation, the AC line current (i_L) is converted by the bridge circuit to DC current (i_d) and passes through LI path. Flowing current through the BFCL diodes, IGBT switch and DC reactor produces some voltage drop and power, which are ignorable. When a fault detects in system, the control system of SBFCL opens the T to insert the limiting-resistor in the fault current flow path. By opening the T in this condition, the i_d passes through the HI path and both i_d and i_L are restricted. Fig. 7 shows the control system of BSFCL, which is designed to improve the LVRT performance of WF under fault scenarios. According to Fig. 7, when the PCC voltage is lower than the threshold value (V_{Th}), the T is opened to put the limiting-resistor in the current flow in fault path.

Sub-Synchronous Resonance

Fig. 8(a) shows the test system including a DFIM connected to grid through compensated line by series capacitor. Fig. 8(b) shows the equivalent-circuit of this system under steady-state grid operation. The resonant frequency of DFIM connected to the compensated transmission-line by a series capacitor is given by following frequency [34]:

(17) $$f_n=f_0\sqrt{\frac{k\sum X}{X_C}}$$

In (17), XC and ∑X represent the series capacitor reactance and the sum of the generator and transmission line inductive reactance. k represents the compensation degree, which is defined as $k=X_C/X_L$. Due to a small disturbance in grid side may cause the currents of frequency f_n to pass through the stator circuit. They can lead to a magnetic-flux of frequency $2\pi f_n$ in the DFIM. This rotating-field induces currents in rotor circuit at following frequency:

(18) $$f_r=f_0-f_n$$

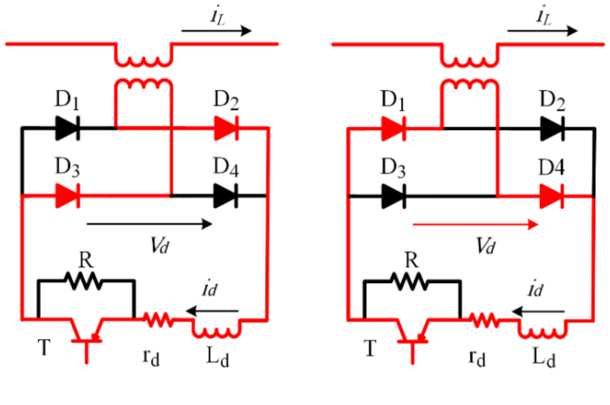

(a) (b)

Fig. 5. Equivalent circuit in normal condition, (a) positive-half cycle, (b) negative-half cycle

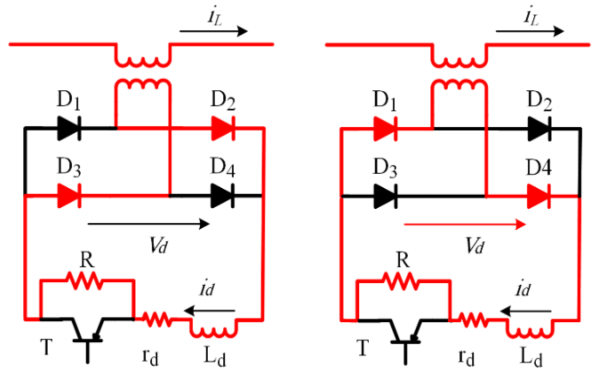

(a) (b)

Fig. 6. Equivalent circuit in fault condition, (a) positive-half cycle, (b) negative-half cycle

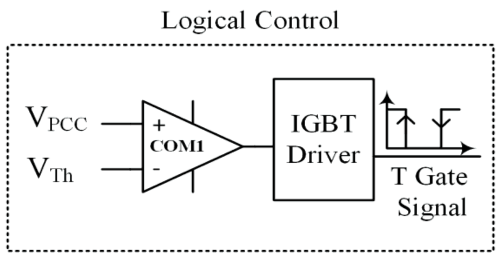

Fig. 7. Control system of the RBFCL

The speed of magnetic field is slower than the electrical speed of rotor. Therefore, f_0-f_n would be negative and would result in the negative equivalent rotor resistance. If this the sum of the DFIM and grid resistance becomes less than the negative resistance, it can lead to the SSR. The SSR phenomena in WFs are classified in two aspects including torque amplification (TA) and self-excitation (SE). The SE phenomena is occurred under steady-state grid condition. The SE phenomena is divided into torsional interaction (TI) and induction-generator effect (IGE) [35-36]. The TA occurs due to short-circuit faults or during switching in grid side.

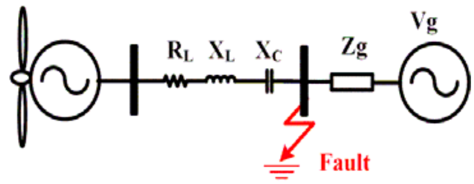

(a)

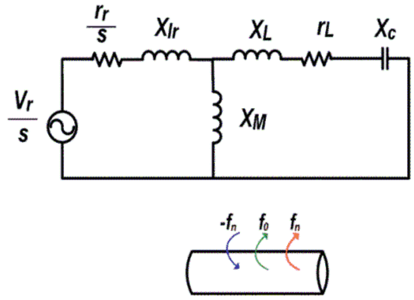

(b)

Fig. 8. (a) Compensated test-system, (b) equivalent circuit of test-system

Simulation Study

To validate the proposed BSFCL capability to damp the SSR in WFs and transmit the max wind power, the system demonstrated in Fig. 4 is utilized. It is modelled and simulated by PSCAD/EMTDC. To capture rated power, the wind speed is regulated at 14m/s. To validate the effectiveness of the BSFCL for SSR damping two different scenarios has been simulated in this study. In scenario 1, the compensation degree is increased from 20% to 70% under steady-state condition. In scenario 2, the compensation degree is set to 50% and a 3-LG fault is simulated in the study system at $t=15s$ and then is cleared after $0.15s$. All simulations for both scenarios are made for cases 1 and 2 as follows:

Case 1: No FCL applied to system
Case 2: By using BSFCL

Scenario 1: Increasing Compensation degree

In this scenario to show the BSFCL performance to damp the SSR, the output power and series compensation level of the WF are adjusted in $P=200MV$ and $k=20\%$. The practical compensation level is limited to 70-75% [37]. In this scenario, the compensation level is changed from 20% to 70% at t=1s. Fig. 9 demonstrates the WF response in scenario 1. Fig. 9(a) demonstrates the out power oscillations for both cases. It is shown that, there are no oscillations for output power in case 2 by using BSFCL unlike case 1. Fig 9(b) demonstrates the DFIM speed in response to increasing the compensation degree. It is observerd from Fig. 9(b), the speed oscillations is effectively damped in case 2, however, the speed osilation is increased in case 1. Fig. 9(c) shows the DFIM torque due to increasing the compensation degree. It is shown that by increasig the compensation degree, the torque osillation is increased in case 1. However, it is effectvely damped in case 2. Fig. 9(d) presents the PCC voltage in this scenario. Considering this figure, the PCC voltage is oscillated by incresing the compensation degree in case 1. However, it is remain constant in case 2 by using the BSFCL. Fig. 10(a) and (b) demonstrates the line current in response to increasing the compensation degree for case1 and case 2, respectively. It is shown that, the line current is oscillatedand increase. However, it is damped in case 2. Fig. 10 (c) and (d) demonstrates the rotor current for case 1 and 2, in this scenario. As shown in this figure, there are no oscillation in rotor currents in case 2.

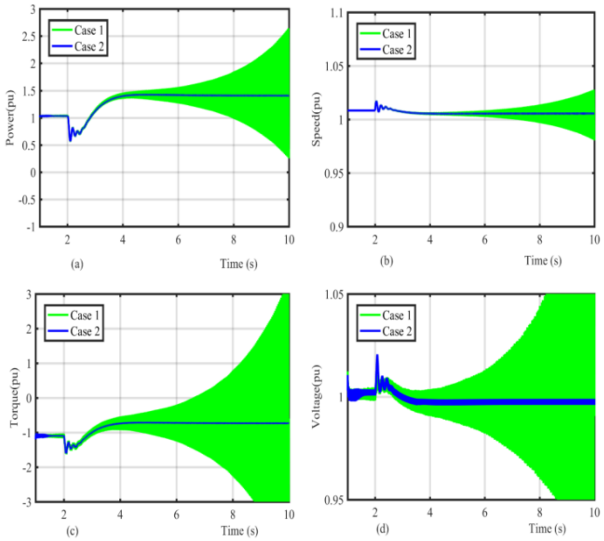

Fig. 9. WF response in scenario 1, (a) output power, (b) Speed, (c) Torque, (d) Voltage

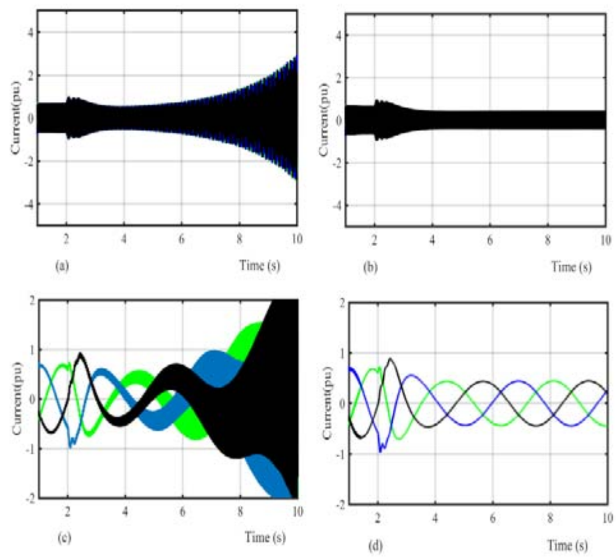

Fig. 10. WF response in scenario 1, (a) Line current in case 1, (b) Line current in case 2, (c) Rotor current in case 1, (d) Rotor current in case 2

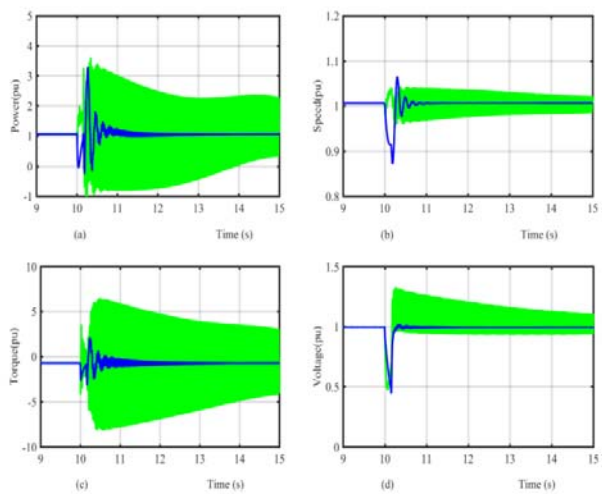

Fig. 11. WF response in scenario 2, (a) output power, (b) Speed, (c) Torque, (d) Voltage

Scenario 2: 3LG Short Circuit Fault

In this scenario to investigate the BSFCL performance to enhance the LVRT and damp the SSR due TA,a 3LG fault is applied at t=10s to the study system shown in Fig. 2 and it is cleared after 0.15s. The output power and series compensation level of the WF are adjusted in P=200MV and k=50%. Also, the wind speed is regulated at 15m/s in this scenario. Fig. 11 demonstrates the WF response to 3LG fault in this scenario.

Fig. 11(a) demonstrates the out power of WF for both cases. It is shown that, the BSFCL effectively mitigate the out put power oscillation in case 2. Fig 11(b) shows the DFIM speed in response to 3LG fault. According to this figure, the speed oscillation is effectively damped in case 2. Fig. 11(c) shows the DFIM torque. It is shown that the BSFCL effectively mitigates the torque osillation in case 2. Fig. 11(d) presents the PCC voltage in this scenario. As presented in this figure, the PCC voltage is reduced to 0.5 pu for both cases due to 3LG fault in study system. In case 1, the PCC voltage starts to oscillate and is damped for long time. In case 2, the PCC voltage recovers to pre-fault level without any oscillations after fault clearance.

Fig. 12(a) and (b) demonstrates the line current in response to 3LG fault for cases 1 and 2, respectively. It is shown that, the line current is oscillated and is increase in case 1. However, it is limited in case 2. Fig. 12(c) and (d) demonstrate the rotor current for cases 1 and 2, in this scenario. By comparing Fig. 12(c) and Fig. 12(d), the rotor current oscillation and over current effectively is dampedin case 2.

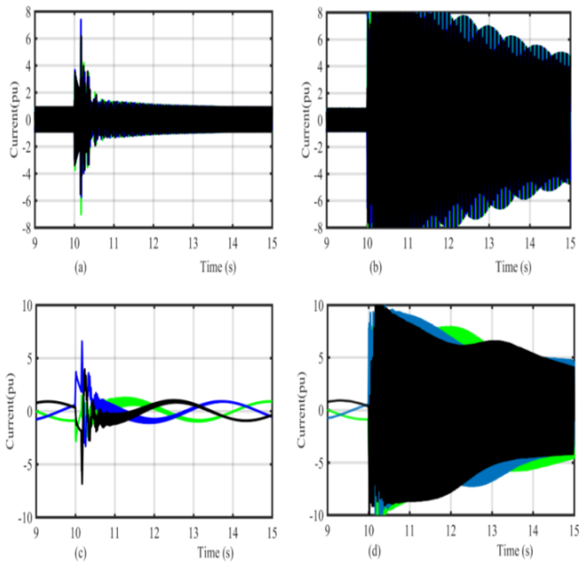

Fig. 12. WF response in scenario 1, (a) Line current in case 1, (b) Line current in case 2, (c) Rotor current in case 1, (d) Rotor current in case 2

Conclusion

This paper proposes the BSFCL application for damping the SSR oscillations due to IGE and TA and enhancing the LVRT capability of a series-capacitor compensated WF equipped with DFIM-based wind turbines. Considering simulation results, the BSFCL effectvely mitigate the SSR osillations in WF even without integration SSR-damping controller and operation of BSFCL control system. Also, it effectively limits fault currets in stator and rotor circuit of DFIM without any oscillation under 3LG fault. Also, It enhances the LVRT performace, when a large disturbance is occurred in the WF.

***Authors**: Yashar Emami, Department of Electrical Engineering, Aliabad Katoul Branch, Islamic Azad University, Aliabad Katoul, Iran. Email: emami_yashar@aliabadiau.ac.ir ; **Corresponding Author:** Dr. Amangaldi Koochaki, Department of Electrical Engineering, Aliabad Katoul Branch, Islamic Azad University, Aliabad Katoul, Iran , E-mail: Koochaki@aliabadiau.ac.ir ; Masoud Radmehr, Department of Electrical Engineering, Aliabad Katoul Branch, Islamic Azad University, Aliabad Katoul, Iran , E-mail: m_radmehr@aliabadiau.ac.ir.*

REFERENCES

[1] Xiaorong Xie,Xu Zhang,Huakun Liu,Hui Liu,Yunhong Li,Chuanyu Zhang, "Characteristic Analysis of Subsynchronous Resonance in Practical Wind Farms Connected to Series-Compensated Transmissions," *IEEE Transactions on Energy Conversion*, **32**, No. 3, 1117-1126, 2017.

[2] A. Moharana; R. K. Varma, "Subsynchronous resonance in single-cage self-excited-induction-generator-based wind farm connected to series-compensated lines," *IET Generation, Transmission & Distribution*, **5**, No. 12, 2011.

[3] M. Tsili and S. Papathanassiou, "A Review of Grid Code Technical Requirements for Wind Farms," *IET Renewable Power Generation*, **3**, No. 3, 308–332, Sept. 2009.

[4] Khaled Mohammad Alawasa; Yasser Abdel-Rady I. Mohamed , "A Simple Approach to Damp SSR in Series-Compensated Systems via Reshaping the Output Admittance of a Nearby VSC-Based System," *IEEE Transactions on Industrial Electronics*, . **62**, No. 5, 2673-2682, 2015.

[5] R. Varma, S. Auddy, Semsedini , "Mitigation of subsynchronous resonance in a series-compensated wind farm using static var compensator Power Eng Soc Gen Meet 2006,*IEEE*, **27**, 1-7

[6] V. Boopathi, R. Muzamil Ahamed, R.P.Kumudini, "Analysis and mitigation of subsynchronous oscillations in a radially-connected wind farm 2014 Power Energy System Conference Towar Sustain Energy, *PESTSE*. 2014, .1–7

[7] Hossein Ali Mohammadpour; Md. Moinul Islam; Enrico Santi; Yong-June Shin, "SSR Damping in Fixed-Speed Wind Farms Using Series FACTS Controllers," *IEEE Transactions on Power Delivery*, Vol. 31, No. 1, pp. 76-86, 2016.

[8] Hossein Ali Mohammadpour; Enrico Santi, "Optimal adaptive sub-synchronous resonance damping controller for a series-compensated doubly-fed induction generator-based wind farm," *IET Renewable Power Generation*, **9,** No. 6, 669-681, 2015.

[9] M. Abdeen et al, "Adaptive Fuzzy Supplementary Controller for SSR Damping in a Series-Compensated DFIG-Based Wind Farm" *IEEE Access*, **5**, No. 4, 1467-1476, Jan 2023.

[10] Sajjad Golshannavaz; Farrokh Aminifar; Daryoush Nazarpour, "Application of UPFC to Enhancing Oscillatory Response of Series-Compensated Wind Farm Integrations"*IEEE Transactions on Smart Grid*, Vol. 11, pp. 1961-1968, 2014.

[11] Li Wang and et al, "Damping of Subsynchronous Resonance in a Hybrid System With a Steam-Turbine Generator and an Offshore Wind Farm Using a Unified Power-Flow Controller" *IEEE Transactions on power System*, Vol. 57, No. 1, pp. 110-120, Feb. 2021

[12] M. Ghorbani, M. Firouzi, B. Mozafari, and F. Golshan, , "Power flow management and LVRT enhancement by using multi-functional capacitive bridge-type fault current limiterisystem" *International Journal of Electrical Power & Energy Systems*, 148, p.108810. 2023

[13] Xiang Zheng; Zheng Xu; Jing Zhang, "A supplementary damping controller of TCSC for mitigating SSR", *2009 IEEE Power & Energy Society General Meeting*, Calgary, AB, Canada, October 2009

[14] R. Varma, S. Auddy, Semsedini , "Mitigation of subsynchronous resonance in a series-compensated wind farm using FACTS controllers," *IEEE Transactions on Power Delivery*, **23**, No. 3, 1645-1654, 2008.

[15] Akshaya Moharana; Rajiv K. Varma; Ravi Seethapathy, "SSR Alleviation by STATCOM in Induction-Generator-Based Wind Farm Connected to Series Compensated Line," *IEEE Transactions on Sustainable Energy*, 5, No. 3, 947-957, 2014.

[16]S. Golshannavaz; M. Mokhtari; D. Nazarpour, "SSR suppression via STATCOM in series compensated wind farm integrations"*2011 19th Iranian Conference on Electrical Engineering*, 1-6, 2011

[17] Ahmed. M. M. Rashad; Salah Kamel, "Enhancement of Hybrid Wind Farm performance using tuned SSSC based on Multi-Objective Genetic Algorithm" *2016 Eighteenth International Middle East Power Systems Conference (MEPCON)*, 786-791, 2016

[18] G.D. Irwin, A .K . Jindal, A .L . Isaacs, "Sub-synchronous control interactions between Type3 wind turbines and series compensated AC transmission system "*IEEE Power Energy Society General Meeting* .2011,p. 1–6. Doi:10.1109/PES.2011.6039426.

[19] K. J. Du, X. Y. Xiao, Y. Wang, Z. X. Zheng, Ch. S. Li, "Enhancing Fault Ride-Through Capability of DFIG-Based Wind Turbines Using Inductive SFCL With Coordinated Control," *IEEE Transactions on Applied Superconductivity*. . **29**, No. 2, March 2019

[20] Hossain MA, Islam MR, Haque MY, Hasan J, Roy TK, Sadi MA. Protecting DFIG-based multi-machine power system under transient-state by nonlinear adaptive backstepping controller-based capacitive BFCL. *IET Generation, Transmission & Distribution*. 2022 Nov;16(22):4528-48.

[21] S. Tohidi S, B.M. Ivatloo, "A comprehensive review of low voltage ride through of doubly fed induction wind generators", Renewable and Sustainable Energy Rev. s, **57,** 412-419, 2016

[22] M. A. Sadi MA, A. A Hussein A, M. A. Shoeb," Transient performance improvement of power systems using fuzzy logic controlled capacitive-bridge type fault current limiter", *IEEE Transactions on Power Systems*, **36**, No. 1, 323-35, 2020.

[23] M. R. Shafiee, et al , "A Dynamic Multi-Cell FCL to Improve the Fault Ride through Capability of DFIG-Based Wind Farms" *Energies*, **13**, No. 22, Nov. 2020

[24] H. Radmanesh, H. Fathi and G. B. Gharehpetian, "Series Transformer-Based Solid State Fault Current Limiter," in *IEEE Transactions on Smart Grid*, 6, no. 4, pp. 1983-1991, July 2015.

[25] Zolfaghari, M. Gilvanejad,G.**B**. Gharehpetian, "A survey on fault current limiters: development and technical aspects" *International Journal of Electrical Power Energy System*, 1**18**, P. 105729, 2020

[26] M Firouzi, "Low-voltage ride-through (LVRT) capability enhancement of DFIG-based wind farm by using bridge-type superconducting fault current limiter (BTSFCL)" *journal of Power Technologies*, **99,** No. 4, 245-253, 2020

[27] O. Alizadeh, A. Yazdani, B. Venkatesh, and B. N. Singh, "Design and transient operation assessment of resonant FCLs in bulk power systems," *IEEE Trans. Power Deliv*., vol. 31, no. 4, 1580–1590, 2016. DOI: 10.1109/ TPWRD.2015.2476704

[28] H. Radmanesh and S. H. Fathi, "Parallel resonance type fault current limiting circuit breaker," in High Voltage, **5**, no. 1, 76-82, 2 2020.

[29] M. Khorasaninejad, et al , "Application of a resistive mutual-inductance fault current limiter in VSC-based HVDC system", *International Journal of Electrical Power & Energy*, **134**, P. 107388, Jan 2022

[30] M. Firouzi, M. R. Shafiee, G. B. Gharehpetian, "Multi-Resistor Bridge-Type FCL for FRT Capability Improvement of DFIG-based Wind Farm" *IET Energy System Integration*. **2**, No. 4, 316-324, Dec 2020

[31] M. A. H. Sadi, A. AbuHussein, M. A. Shoeb, "Transient Performance Improvement of Power Systems Using Fuzzy Logic Controlled Capacitive-Bridge Type Fault Current Limiter," *IEEE Transactions on Power Systems*, **36,** No.1, Jan. 2021

[32] G. Rashid, and M. H. Ali, "Transient Stability Enhancement of Double Fed Induction Machine Based Wind Generator by Bridge-Type Fault Current Limiter," *IEEE Transactions on Energy Conversion* , Vol. 30, No. 3, 2015.

[33] P. M. Anderson and Anjan Bose, "Stability Simulation of Wind Turbine Systems," *IEEE Transactions on Power Apparatus and Systems*, . PAS-102, No.12, 3791-3795, Dec 1983

[34] H. Nian, Y. Xu, L. Chen and M. Zhu, "Modeling and Analysis of DC Link Dynamics in DFIG System With an Indicator Function," in *IEEE Access*, **7**, 125401-125412, 2019, doi: 10.1109/ACCESS.2019.2938796.

[35] C. Zhang, X. Cai, M. Molinas and A. Rygg, "Frequency-domain modelling and stability analysis of a DFIG-based wind energy conversion system under non-compensated AC grids: impedance modelling effects and consequences on stability," in *IET Power Electronics*, **12,** no. 4, 907-914, 10 4 2019, doi: 10.1049/ietpel.2018.5527

[36] A. Rygg, M. Molinas, C. Zhang and X. Cai, "A Modified Sequence Domain Impedance Definition and Its Equivalence to the dq-Domain Impedance Definition for the Stability Analysis of AC Power Electronic Systems," in *IEEE Journal of Emerging and Selected Topics in Power Electronics*, **4**, no. 4, 1383-1396, Dec. 2016

[37] Y. Zhang, C. Klabunde and M. Wolter, "Study of Resonance Issues between DFIG-based Offshore Wind Farm and HVDC Transmission," in Proceeding of Power System Computation *Conference 2020, Porto, Portugal*, 2020, also to be included in a special issue of the journal Electric Power Systems Research (EPSR)